

Green Chemistry

Accepted Manuscript



This article can be cited before page numbers have been issued, to do this please use: L. Zhang, R. K. Singh, S. D. Z. Guo, J. Li, F. Chen, Y. He, X. Guan, Y. C. Kang and J. Lee, *Green Chem.*, 2017, DOI: 10.1039/C7GC02898A.



This is an Accepted Manuscript, which has been through the Royal Society of Chemistry peer review process and has been accepted for publication.

Accepted Manuscripts are published online shortly after acceptance, before technical editing, formatting and proof reading. Using this free service, authors can make their results available to the community, in citable form, before we publish the edited article. We will replace this Accepted Manuscript with the edited and formatted Advance Article as soon as it is available.

You can find more information about Accepted Manuscripts in the [author guidelines](#).

Please note that technical editing may introduce minor changes to the text and/or graphics, which may alter content. The journal's standard [Terms & Conditions](#) and the ethical guidelines, outlined in our [author and reviewer resource centre](#), still apply. In no event shall the Royal Society of Chemistry be held responsible for any errors or omissions in this Accepted Manuscript or any consequences arising from the use of any information it contains.

**Artificial synthetic pathway for acetoin, 2,3-butanediol, and
2-butanol production from ethanol using cell free multi-enzyme
catalysis †**

Liaoyuan Zhang*,^{a,b,†} Raushan Singh,^{b,†} Sivakumar D,^b Zewang Guo,^a Jiahuan Li,^a
Fanbin Chen,^a Yuanzhi He,^a Xiong Guan,^a Yun Chan Kang,^{*,c} and Jung-Kul Lee^{*,b}

^aKey Laboratory of Biopesticide and Chemical Biology, Ministry of Education, College of Life Sciences, Gutian Edible Fungi Research Institute, Fujian Agriculture and Forestry University, Fuzhou, Fujian province, 350002, PR China

^bDepartment of Chemical Engineering, Konkuk University, Seoul 05029, Republic of Korea

^cDepartment of Materials Science and Engineering, Korea University, Seoul 02841, Republic of Korea

†: These authors contributed equally to this work.

*Corresponding author: Key Laboratory of Biopesticide and Chemical Biology, Fujian Agriculture and Forestry University, Ministry of Education, FuZhou, Fujian Province, 350002, PR China Tel.: +86-591-83789492; Fax: +86-591-83789121;
E-mail: zliaoyuan@126.com

*Corresponding author: Department of Materials Science and Engineering, Korea University, Seoul 143-701, Republic of Korea Tel.: +82-2-4503505; Fax: +82-2-4583504;
E-mail: yckang@korea.ac.kr

*Corresponding author: Department of Chemical Engineering, Konkuk University, Seoul 05029, Republic of Korea Tel.: +82-2-4503505; Fax: +82-2-4583504;
E-mail: jkrhee@konkuk.ac.kr

† Electronic supplementary information

1 **Abstract**

2 Upgrading ethanol to higher order alcohols is desired but difficult by using
3 current biotechnological methods. In this study, we designed a completely artificial
4 reaction pathway for upgrading ethanol to acetoin, 2,3-butanediol, and 2-butanol in a
5 cell-free bio-system composed of ethanol dehydrogenase, formolase, 2,3-butanediol
6 dehydrogenase, diol dehydratase, and NADH oxidase. Under optimized conditions,
7 acetoin, 2,3-butanediol, and 2-butanol were produced at 88.78%, 88.28%, and 27.25%
8 of the theoretical yield from 100 mM ethanol, respectively. These results demonstrate
9 an environment-friendly novel approach for upgrading bio-ethanol to acetoin,
10 2,3-butanediol, and 2-butanol.

11

12 Introduction

13 The production of biofuels from renewable biomass has been given increased
14 attention because of the finite supply of fossil fuels.¹⁻³ It is estimated that the global
15 biofuel market consists of approximately 15% biodiesel and 85% bioethanol.^{4,5}
16 Bioethanol, a direct product of biomass fermentation, is considered a renewable
17 energy source that can replace or blend with gasoline for transportation use.^{6,7}
18 Gasoline blended with the appropriate bioethanol as a fuel additive may increase the
19 octane level and reduce toxic emissions of pollutants.⁸ However, several
20 disadvantages including the low energy density, high hygroscopicity, and corrosivity
21 to engine technology and fuel pipelines limit the broad implementation of bioethanol
22 in global transportation.^{7,9,10} This has shifted research interests to higher-order
23 alcohols such as 2,3-butanediol and butanol.^{7,11,12}

24 2,3-Butanediol is an important platform chemical and potential aviation fuel with
25 a heating value of 27.2 kJ g⁻¹ and can be used to produce butadiene (a monomer of
26 synthetic rubber), acetoin (a volatile compound used in foods, plant growth promoters,
27 and biological pest controls), diacetyl (a flavor enhancer), and methyl ethyl ketone
28 (2-butanone, an excellent organic solvent).¹³⁻¹⁵ Furthermore, 2-butanone can be
29 hydrogenated to produce 2-butanol, which shows the highest octane number and
30 lowest boiling point among the four stereoisomers of butanol.^{1,16} Compared to
31 bioethanol, butanol has a higher energy density and lower hygroscopicity and can be
32 directly blended with gasoline without the need for modifying current vehicle
33 system.^{17,18} In recent years, many studies have been conducted to engineer microbes
34 for 1-butanol and isobutanol production through genetic modifications.^{19,20} However,
35 bio-production of 2-butanol has not been widely explored. Few studies of 2-butanol
36 production have been conducted by extending the terminal product of 2,3-butanediol

37 or acetolactate using metabolic engineering methods.^{1,16,21} The final 2-butanol
38 concentration was still quite low because of metabolic flux limitations and its
39 inevitable toxicity to microbial cells.

40 One of the potential solutions for overcoming these limitations is to construct a
41 simplified pathway *in vitro* using a limited number of enzymes, a process known as
42 cell-free metabolic engineering (CFME). CFME is a cell-free bio-system that uses *in*
43 *vitro* ensembles of catalytic proteins prepared from purified enzymes or crude lysates
44 of cells to produce target products.^{22,23} It can efficiently eliminate cell-associated
45 process barriers, such as substrate or product toxicity, intracellular flux balance that
46 results in low target product yield and unwanted by-products, and product excretion
47 constraints by intracellular transport barriers.^{4,22,24} Compared with traditional
48 metabolic engineering, CFME has many unique advantages including no requirement
49 for cell growth, shorter synthetic pathway, faster reaction rate, higher theoretical yield
50 and productivity, and easier manipulation of reaction conditions, although some
51 challenges such as activity, stability, and cost of enzymes must be resolved.^{25,26}

52 The costs of acetoin (10,000–30,000 \$/ton), 2,3-butanediol (10,000–50,000
53 \$/ton), and 2-butanol (10,000–78,000 \$/ton) are over 10-fold that of ethanol (800–950
54 \$/ton), according to the global trade data (www.alibaba.com). To upgrade ethanol to
55 higher-order alcohols, we designed a completely artificial CFME-based reaction
56 pathway composed of ethanol dehydrogenase, formolase, 2,3-butanediol
57 dehydrogenase, diol dehydratase, and NADH oxidase for the conversion of ethanol
58 into C₄ alcohols. Furthermore, protein engineering was conducted to improve the
59 catalytic efficiencies of formolase and diol dehydratase to increase the conversion rate
60 of this artificial pathway. In addition, a novel NAD(P)H purge valve regulatory node
61 was developed to prevent NADH buildup in the artificial reaction. The results showed

62 that C₄ compounds including acetoin, 2,3-butanediol, and 2-butanol can be efficiently
63 produced from ethanol using the CFME-based artificial reaction pathway.

64

65 **Experimental**

66 **Enzymes and chemicals**

67 Restriction enzymes, DNA Polymerase High Fidelity and T₄ DNA ligase, were
68 purchased from TaKaRa Biotech (Shiga, Japan) and New England Biolabs (Ipswich,
69 MA, USA), respectively. DNA and protein markers were obtained from Tiangen
70 Biotech (Shanghai, China). Isopropyl-beta-D-thiogalactopyranoside (IPTG),
71 dithiothreitol (DTT), and dimethyl sulfoxide (DMSO) were purchased from
72 Sigma-Aldrich (St. Louis, MO, USA) and Sinopharm (Shanghai, China), respectively.
73 The standards, including (3*S*/3*R*)-acetoin, (2*S*,3*S*)-2,3-butanediol, (2*R*,3*R*)-2,3-
74 butanediol, *meso*-2,3-butanediol, butanone, and 2-butanol, were obtained from
75 Sigma-Aldrich. All other chemicals, unless otherwise indicated, were of analytical
76 grade and commercially available.

77

78 **Bacterial strains, plasmids, and bacterial growth conditions**

79 The strains and plasmids used in this study are presented in [Table 1](#). *Escherichia*
80 *coli* DH5 α and BL21(DE3) as the cloning and expression hosts were cultured at 37°C.
81 The plasmid pET28a was used to construct the expression vector. Luria-Bertani (LB)
82 medium was used for strain cultivation and recombinant protein expression.
83 Kanamycin was added to the LB medium for cultivation of recombinant strains at a
84 final concentration of 50 $\mu\text{g mL}^{-1}$.

85

86 **Recombinant proteins expression and purification**

87 The genes for ethanol dehydrogenase (EtDH), formolase (FLS), 2,3-butanediol
88 dehydrogenase (BDH), and diol dehydratase (DDH), and NADH oxidase (NOX) from
89 *Cupriavidus necator*,²⁷ *Pseudomonas fluorescens*,²⁸ *Clostridium autoethanogenum*,²⁹
90 *Lactobacillus brevis*,^{1,30} and *Lactobacillus rhamnosus*³¹ were synthesized by General
91 Biosystems, Inc. (Anhui, China) and cloned into the expression plasmid pET28a (The
92 details of enzyme sequences are presented in the ESI). The protein expression
93 plasmids were introduced into *E. coli* BL21(DE3). Recombinant *E. coli* BL21(DE3)
94 harboring pET-EtDH, pET-FLS, pET-BDH, pET-DDH, pET-dhaR, pET-DDH-dhaR,
95 and pET-NOX were cultured at 37°C in LB medium and induced by adding 0.5 mM
96 IPTG when the optical density was 0.6 at 600 nm. After induction for 24 h at 18°C,
97 the cells were harvested by centrifugation and disrupted by sonication in an ice bath.
98 The cell lysate was centrifuged at 8000 ×g for 10 min to remove the cell debris. For
99 the EtDH, FLS, BDH, dhaR, and NOX enzymes, the soluble fraction was subjected to
100 purification with a HisTrap HP column according to the purification protocol (GE
101 Healthcare, Little Chalfont, UK). DDH purification was carried out as described
102 previously.³² The purified enzymes were concentrated and desalted by ultrafiltration,
103 and then detected by SDS-PAGE.

104

105 **Development of the enzyme variants**

106 The EtDH:D46G and BDH:S199A variants were generated by site-directed
107 mutagenesis, which was performed using the primers EtDH1/EtDH2 and
108 BDH1/BDH2 as shown in [Table S1†](#). The recombinant plasmids pET-EtDH and
109 pET-BDH containing the wild-type EtDH and BDH genes were used as DNA
110 templates for PCR-amplification, respectively. Recombinant plasmids harboring the
111 correct mutant genes were transformed into *E. coli* BL21(DE3) and colonies selected

112 via kanamycin resistance were used for protein expression. After purification, the
113 activities and kinetic parameters of the EtDH and BDH variants were determined.

114 To improve the catalytic efficiency of the FLS enzyme, the HotSpot Wizard 2.0
115 server was used to analyze hot spots by inputting the FLS structure (PDB No.:
116 4QPZ).^{28,33} Six residuals as hot spots (T396, T446, M473, S477, L482, and L499)
117 were identified and subjected to site-saturated mutagenesis using the primers
118 FLS1–FLS12 (Table S1†). The recombinant plasmid pET-FLS containing the
119 wild-type FLS gene was used as a DNA template. Recombinant plasmids containing
120 the mutant genes were transformed into *E. coli* BL21(DE3). FLS variants were
121 screened using the whole-cell biocatalytic method with acetaldehyde as a substrate.
122 Briefly, the colonies were inoculated in LB medium and protein expression was
123 induced by adding 0.5 mM IPTG for 24 h at 18°C when the optical density at 600 nm
124 reached 0.6. The cells were harvested by centrifugation and used to carry out
125 whole-cell biocatalysis in a reaction mixture containing 50 mM phosphate buffer (pH
126 8.0), 100 mM acetaldehyde, and 40 g L⁻¹ wet cell weight (WCW) at 30°C for 6 h. The
127 product acetoin was quantified using the Voges-Proskauer (VP) reaction (See the ESI).
128 Moreover, positive variants were verified by enzyme activity and kinetic parameter
129 assays after purification. Variants were also analyzed by commercial sequencing.

130 DDH variants including S302A, Q337A, F375I, S302A/Q337A, S302A/F375I,
131 Q337A/F375I, and S302A/Q337A/F375I were developed to assess their catalytic
132 efficiencies compared with the wild-type DDH enzyme. Site-directed mutagenesis
133 was performed using the primers DDH1-DDH6 as shown in Table S1†. The
134 recombinant plasmid pET-DDH-dhaR harboring the wild-type DDH and its
135 reactivating factor dhaR genes were used as DNA templates for PCR amplification.
136 The PCR products were transformed into *E. coli* BL21(DE3) for protein expression,

137 which was conducted in LB medium containing 0.5 mM IPTG at 18°C for 24 h. These
138 variants were used to evaluate the catalytic activities using whole-cell biocatalysis
139 with *meso*-2,3-butanediol as a substrate. The reaction mixture consisted of 50 mM
140 HEPES buffer (pH 7.0), 50 mM *meso*-2,3-butanediol, 20 μ M coenzyme B₁₂, and 40 g
141 L⁻¹ wet cell weight, and whole-cell biocatalysis was carried out at 30°C for 6 h in the
142 dark. The product butanone was analyzed and quantified by gas chromatography.

143

144 **Enzyme activity assays**

145 EtDH activity: The activities of EtDH and its variant were determined in a
146 reaction mixture containing 100 mM glycine-NaOH buffer (pH 9.5), 5 mM Mg²⁺, 3
147 mM NAD⁺/NADP⁺, and 10 mM ethanol at 25°C. The activity was defined by the
148 reduction rate of NAD⁺/NADP⁺ at 340 nm using a spectrophotometer (UV-1800,
149 MAPADA, Shanghai, China). One unit of EtDH activity was defined as the amount of
150 enzyme required to reduce 1 μ mol of NAD⁺/NADP⁺ per minute.

151 FLS activity: The activities of FLS and its variants were assayed in a reaction
152 mixture containing 100 mM phosphate buffer (pH 8.0), 1 mM Mg²⁺, 0.1 mM TPP, and
153 20 mM acetaldehyde. After the reaction was conducted at room temperature for 1 h,
154 acetoin concentration from acetaldehyde was determined by the VP reaction and
155 calculated from calibration curves of standard acetoin. One unit of FLS activity was
156 defined as the amount of enzyme that produced 1 μ mol acetoin from acetaldehyde per
157 minute.

158 BDH activity: The activities of BDH and its variant were measured in a reaction
159 mixture containing 50 mM Tris-HCl buffer (pH 7.5), 0.2 mM NADPH, 1 mM DTT,
160 and 20 mM acetoin or 5 mM butanone at room temperature. The activity was defined
161 by the oxidation rate of NADPH at 340 nm using a spectrophotometer (UV-1800,

162 MAPADA). One unit of BDH activity was defined as the amount of enzyme required
163 to oxidize 1 μmol of NADPH per minute.

164 DDH activity: The activities of DDH and its variants with its reactivating factor
165 dhaR were determined in a reaction mixture containing 50 mM phosphate buffer (pH
166 7.0), 1 mM coenzyme B₁₂, 100 mM ATP, 1 mM Mg²⁺, and 50 mM
167 *meso*-2,3-butanediol. After conversion at room temperature in the dark for 1 h, the
168 reaction was stopped by adding an equal volume of citrate buffer (100 mM, pH 3.6).
169 The product butanone was detected and quantified by gas chromatography. One unit
170 of DDH activity was defined as the amount of enzyme that produces 1 μmol butanone
171 from *meso*-2,3-butanediol per minute.

172 NOX activity: The NOX activity was determined in a reaction mixture
173 containing 50 mM HEPES-NaOH buffer (pH 8.0) and 0.2 mM NADH at room
174 temperature. The activity was defined by the oxidation rate of NADH at 340 nm using
175 a spectrophotometer (UV-1800, MAPADA). One unit of NOX activity was defined as
176 the amount of enzyme required to oxidize 1 μmol of NADH per minute.

177

178 **Determination of kinetic parameters**

179 The kinetic parameters of EtDH and EtDH:D46G were determined in a reaction
180 mixture containing 100 mM glycine-NaOH buffer (pH 9.5), 5 mM Mg²⁺, 3 mM
181 NAD⁺/NADP⁺, and 0.5-100 mM ethanol at room temperature. The K_m and k_{cat} values
182 were obtained by nonlinear regression fitting of the Michaelis-Menten equation. All
183 assays were carried out in triplicate.

184 The kinetic parameters of FLS and its variants were assayed in a reaction mixture
185 containing 100 mM phosphate buffer (pH 8.0), 1 mM Mg²⁺, 0.1 mM TPP, and 0.5-20
186 mM acetaldehyde at room temperature. The K_m and k_{cat} values were obtained by

187 nonlinear regression fitting of the Michaelis-Menten equation. All assays were carried
188 out in triplicate.

189 The kinetic parameters of BDH and BDH:S199A were measured in a reaction
190 mixture containing 50 mM Tris-HCl buffer (pH 7.5), 0.2 mM NADPH, 1 mM DTT,
191 and 0.5-100 mM acetoin or 0.5–10 mM butanone at room temperature. The K_m and
192 k_{cat} values were obtained by nonlinear regression fitting of the Michaelis-Menten
193 equation. All assays were carried out in triplicate.

194

195 **Cell-free multi-enzyme catalysis system**

196 The synthesis of acetoin, 2,3-butanediol, and 2-butanol from ethanol by cell-free
197 multi-enzyme catalysis was conducted in a 0.5-mL reaction mixture containing
198 substrate, coenzymes, metal ions, and the corresponding enzymes. The reaction
199 conditions including temperature, pH, coenzyme, and metal ions were optimized to
200 improve the flux of the artificial reaction pathway ([See the ESI](#)). The optimal reaction
201 conditions for acetoin, 2,3-butanediol, and 2-butanol from ethanol were as follows.

202 Acetoin production was carried out in a 0.5-mL reaction mixture containing 50
203 mM HEPES buffer (pH 8.0), 1 mM NAD^+ , 0.1 mg mL⁻¹ EtDH, 0.2 mg mL⁻¹
204 FLS:L482S, 0.1 mg mL⁻¹ NOX, 0.1 mM TPP, 1 mM Mg^{2+} , 1 mM DTT, 20 % DMSO,
205 and 100 mM ethanol. The reaction was conducted at 30 °C.

206 2,3-Butanediol was produced in a 0.5-mL reaction mixture containing 50 mM
207 HEPES buffer (pH 8.0), 1 mM NAD^+ , 1 mM $NADP^+$, 0.1 mg mL⁻¹ EtDH:D46G, 0.2
208 mg mL⁻¹ FLS:L482S, 0.1 mg mL⁻¹ NOX, 0.1 mg mL⁻¹ BDH:S199A, 0.1 mM TPP, 1
209 mM Mg^{2+} , 1 mM DTT, 20 % DMSO, and 100 mM ethanol. The reaction was
210 conducted at 30 °C.

211 2-Butanol was produced in a 0.5-mL reaction mixture containing 50 mM HEPES

212 buffer (pH 8.0), 1 mM NAD⁺, 1 mM NADP⁺, 0.1 mg mL⁻¹ EtDH:D46G, 0.2 mg mL⁻¹
213 FLS:L482S, 0.1 mg mL⁻¹ NOX, 0.1 mg mL⁻¹ BDH:S199A, 0.2 mg mL⁻¹
214 DDH:Q337A/F375I, 0.2 mg mL⁻¹ dhaR, 0.1 mM TPP, 1 mM Mg²⁺, 1 mM DTT, 20 %
215 DMSO, 1 mM coenzyme B₁₂, 100 mM ATP, and 100 mM ethanol. The reaction was
216 carried out at 30 °C.

217 All reactions were carried out for 6 h and the products were identified by
218 gas chromatography (GC). The product percentage yields were calculated using the
219 following equation: percentage yield (%) = product yield (mM)/theoretical yield
220 (mM). Theoretically, two moles of ethanol can generate one mole of acetoin or
221 2,3-butanediol or 2-butanol.

222

223 **Recyclability of cascade reactions**

224 Purified enzymes were mixed with activated silicon oxide nanoparticles and
225 incubated for 12 h at 4°C. Before immobilization, the silicon oxide nanoparticles
226 (4830HT; Nanostructured & Amorphous Materials, Houston, TX, USA) were
227 activated by treating the nanoparticles with glutaraldehyde (Sigma). Immobilization
228 yield (%) and immobilization efficiency (%) were calculated for the immobilized
229 enzymes as follows: immobilization efficiency = $(\alpha_i/\alpha_f) \times 100$, immobilization yield =
230 $[\{P_i - (P_w + P_s)\} / P_i] \times 100$, where α_i is the total activity of the immobilized enzyme and
231 α_f is the total activity of the free enzyme. P_i is the total protein content of the crude
232 enzyme preparation and P_w and P_s are the protein concentrations in the wash solution
233 and supernatant after immobilization, respectively.

234 For acetoin production, the reaction was performed in a 0.5-mL reaction mixture
235 containing 50 mM HEPES buffer (pH 8.0), 1 mM NAD⁺, 1.06 U mL⁻¹ EtDH, 0.05 U
236 mL⁻¹ FLS:L482S, 0.98 U mL⁻¹ NOX, 0.1 mM TPP, 1 mM Mg²⁺, 1 mM DTT, 20%

237 DMSO, and 100 mM ethanol. Similarly, 2,3-butanediol production was performed in
238 a 0.5-mL reaction mixture containing 50 mM HEPES buffer (pH 8.0), 1 mM NAD⁺, 1
239 mM NADP⁺, 0.1 mg mL⁻¹ EtDH:D46G, 0.2 mg mL⁻¹ FLS:L482S, 0.1 mg mL⁻¹ NOX,
240 0.1 mg mL⁻¹ BDH:S199A, 0.1 mM TPP, 1 mM Mg²⁺, 1 mM DTT, 20% DMSO, and
241 100 mM ethanol. The reaction was conducted at 30°C for 6 h. The reusability of
242 immobilized enzymes was examined under the same reaction conditions. After each
243 reaction cycle, the immobilized enzyme was removed by centrifugation at 4000 ×g for
244 30 min. The immobilized enzyme was collected and washed with deionized water and
245 buffer. For the second reaction cycle, the immobilized enzyme was dissolved in fresh
246 buffer, added to the substrate, and processed as in the first cycle.

247

248 **Analytical methods**

249 Cell growth was determined by measuring the optical density at 600 nm with a
250 spectrophotometer (UV-1800, MAPADA). Protein concentration was determined
251 using the Bradford method, and bovine serum albumin served as the standard protein.
252 The concentrations of ethanol, acetaldehyde, acetoin, 2,3-butanediol, butanone, and
253 2-butanol were determined with the addition of isoamylol as an internal standard and
254 quantified using a gas chromatograph system (Agilent GC9860, Santa Clara, CA,
255 USA) equipped with a chiral column (Supelco β-DEX™ 120, 30-m length, 0.25-mm
256 inner diameter). The operation conditions were as follows: N₂ was used as the carrier
257 gas at flow rate of 1.2 mL min⁻¹; injector temperature and detector temperature were
258 215 and 245°C, respectively; and column temperature was maintained at 50°C for 1.5
259 min, and then increased to 180°C at a rate of 15°C min⁻¹.

260

261

262 Results and discussion

263 Construction of artificial pathway for C₄ compound production from ethanol

264 We designed a novel artificial reaction pathway for the conversion of ethanol into
265 the C₄ compounds acetoin, 2,3-butanediol, and 2-butanol, which required cascade
266 enzymes (Fig. 1). Ethanol is first dehydrogenated by the NAD(P)H-dependent EtDH
267 to afford acetaldehyde, which undergoes a condensation reaction to yield acetoin by
268 FLS, a computationally designed enzyme. Subsequently, acetoin is reduced by the
269 NADPH-dependent BDH to produce 2,3-butanediol. Finally, 2-butanol is obtained via
270 dehydration and hydrogenation reaction by DDH and BDH, respectively. NOX is used
271 to regenerate NAD⁺ throughout the reaction process. Considering that oxygen is used
272 as a substrate for NOX, aeration may be required for a large-scale reaction. By
273 stoichiometry, 1 M ethanol is converted completely into acetoin or 2,3-butanediol and
274 generates 1 or 0.5 M NADH, respectively, which requires 0.5 M oxygen for acetoin
275 production or 0.25 M oxygen for 2,3-butanediol production (1 M NADH oxidized by
276 NOX requires 0.5 M oxygen as a substrate). Thus, 1 L of the reaction mixture
277 containing 1 M ethanol as a substrate requires 11.2 or 5.6 L oxygen for acetoin or
278 2,3-butanediol production throughout the reaction process. For 2-butanol production,
279 the oxygen demand in the reaction was lower than that of 2,3-butanediol production.
280 Compared to traditional fermentation, the aeration demand in the current reaction
281 system is much lower supporting the scale-up potential of the artificial reaction
282 pathway. In this artificial reaction pathway, we chose EtDH from *C. necator*,²⁷ BDH
283 from *C. autoethanogenum*,²⁹ DDH from *L. brevis*^{1,30} with its reactivating factor dhaR,
284 and NOX enzymes from *L. rhamnosus*³¹ as candidate enzymes because of their
285 relatively high catalytic efficiencies for their corresponding substrates as
286 demonstrated in previous studies. However, the FLS enzyme was only reported to

287 catalyze three molecules of formaldehyde into one molecule of dihydroxyacetone.²⁸
288 To verify the catalytic ability of acetaldehyde conversion to acetoin by the FLS
289 enzyme, the catalytic reaction was carried out using whole-cell biocatalyst
290 over-expressing FLS with acetaldehyde as a substrate. The VP test and GC/GC-MS
291 analysis indicated that racemic acetoin ((3*S*)-acetoin and (3*R*)-acetoin) was produced
292 from acetaldehyde, demonstrating that the FLS enzyme can catalyze the conversion of
293 acetaldehyde into acetoin (Fig. S1†, Fig. S14† and Fig. S15†). These results show that
294 C₄ compounds including acetoin, 2,3-butanediol, and 2-butanol can be produced from
295 ethanol using the artificial reaction pathway.

296

297 **Characterization of enzymes in the artificial pathway**

298 Furthermore, to determine the catalytic efficiencies of these enzymes in the
299 artificial pathway, we systematically determined the kinetic parameters of EtDH, FLS,
300 BDH, and DDH after purification (The results of enzyme expression and purification
301 are presented in the ESI, Fig. S2†, and Fig. S3†). As shown in Table 2, the k_{cat}/K_m
302 values of EtDH for ethanol with NAD⁺, FLS for acetaldehyde with TPP, and BDH for
303 acetoin/butanone with NADPH were 17.09, 7.69×10^{-3} , 18.50, and 19.31 s⁻¹ mM⁻¹,
304 respectively. However, purified DDH enzyme with its reactivating factor dhaR
305 showed low activity (0.02 U mg⁻¹) towards *meso*-2,3-butanediol as a substrate, partly
306 because of its low stability.³² A whole-cell catalytic method was used to determine the
307 conversion of three 2,3-butanediol isomers (*meso*-2,3-butanediol, (2*R*,
308 3*R*)-2,3-butanediol, and (2*S*, 3*S*)-2,3-butanediol) to butanone by *E. coli*/
309 pET-DDH-dhaR cells. The results showed that 20.56 mM butanone was produced
310 from 50 mM *meso*-2,3-butanediol after 6 h (Fig. S4†), indicating that the DDH
311 enzyme with dhaR had high catalytic activity towards *meso*-2,3-butanediol *in vivo*. In

312 contrast, no butanone was detected during whole-cell catalysis in the presence of (2*R*,
313 3*R*)-2,3-butanediol and (2*S*, 3*S*)-2,3-butanediol as substrates (Fig. S4†). These results
314 are consistent with those of a previous study showing that only *meso*-2,3-butanediol
315 was dehydrated by DDH enzyme.³⁴ The enzyme thermostability assay showed that the
316 three enzymes had relatively higher stabilities and retained 87.91% (EtDH), 70.43%
317 (FLS), and 91.30% (NOX) of their initial activities after incubation at 30°C for 6 h,
318 while all enzymes except NOX showed decreased stability at 37 and 45°C (Fig. S5†).

319

320 Acetoin production from ethanol via artificial pathway

321 **Rate limiting step for acetoin production from ethanol.** To test the viability of
322 the artificial pathway, we first investigated acetoin production from ethanol using
323 three enzymes, EtDH, FLS, and NOX, as presented in Fig. 1A. The initial reaction
324 was carried out in a 0.5-mL reaction mixture containing 50 mM HEPES buffer (pH
325 7.0), 0.1 mg mL⁻¹ EtDH, 0.2 mg mL⁻¹ FLS, 0.1 mg mL⁻¹ NOX, 4 mM NAD⁺, 0.1 mM
326 TPP, 1 mM Mg²⁺, 1 mM DTT, 20% DMSO, and 100 mM ethanol as the starting
327 substrate. The reaction was conducted at 30°C for 6 h and 17.98 mM of acetoin at
328 35.96% of the theoretical yield was generated in the reaction solution after 6 h,
329 suggesting that the reaction pathway for upgrading ethanol to acetoin is feasible.
330 Further, the reaction conditions including temperature, pH, coenzyme (NAD⁺ and
331 TPP), and metal ions were optimized to improve the reaction flux from ethanol to
332 acetoin. The optimal reaction conditions including temperature (30°C), pH (8.0),
333 NAD⁺ (1 mM), TPP (0.1 mM), and Mg²⁺ (1 mM) were determined (Fig. S6†). Under
334 the optimized conditions, 22.75 mM of acetoin at 45.50% of the theoretical yield was
335 produced from ethanol (100 mM) after 6 h (Fig. S7†). To determine the rate-limiting
336 step in the reaction, the reaction pathway was systematically reconstituted with 1/10

337 the starting amount of each enzyme, while the other enzymes were kept constant. The
338 results are shown in Fig. 2. For EtDH and NOX, lowering the concentration to 10%
339 had minimal effects on the production of acetoin from ethanol. The exception was
340 FLS, indicating that FLS represents potential bottlenecks.

341 **Engineering of FLS to improve its activity.** To improve the catalytic
342 efficiency of the FLS enzyme, mutational hotspots in the FLS amino acid sequence
343 were analyzed using the HotSpot Wizard 2.0 server.³³ Six hot spot residues (T396,
344 T446, M473, S477, L482, and L499) were identified and altered by site-saturated
345 mutagenesis (Fig. S8†). The results revealed that site 482 in FLS plays an important
346 role in enzyme activity. The FLS variants L482S, L482R, and L482E showed specific
347 activity increases of 59.03%, 36.89%, and 34.12%, respectively (Fig. 3 and Table
348 S2†). Furthermore, the kinetic parameters of the three FLS variants were assayed
349 using the substrate acetaldehyde with TPP as a coenzyme. The k_{cat}/K_m values of the
350 FLS variants L482S, L482R, and L482E for acetaldehyde were 1.33×10^{-2} , $1.06 \times$
351 10^{-2} , and 9.66×10^{-3} with improvements of 72.95%, 37.84%, and 25.62%,
352 respectively, compared to wild-type FLS (Table 2).

353 The mutant FLS:L482S showed higher activity than wild-type FLS.
354 Computational studies for FLS variants at atomic resolution using molecular
355 dynamics simulation for 100 ns provided insight into the structural changes for the
356 mutation L482S and its correlation with enzymatic activity. Computational analysis
357 revealed that W480 in the mutant FLS:L482S made stronger contacts (2.1Å) with the
358 substrate acetaldehyde than the wild-type (2.8Å) (Fig. S9A-B†). Siegel *et al* (2015)
359 reported W480 as an active site residue in FLS (4QPZ), supporting the higher activity
360 of FLS:L482S.²⁸ The 100-ns molecular dynamics analysis also shows that the
361 FLS:L482S retained more hydrogen bond contacts than the wild-type enzyme (Fig.

362 S9C-D†).

363 **Acetoin production from ethanol using mutant FLS:L482S** The FLS:L482S
364 rather than the wild-type enzyme was used to conduct the reaction from ethanol to
365 acetoin under optimized reaction conditions. As shown in Fig. 4A, a maximum
366 concentration of acetoin (44.39 mM) was obtained from ethanol (100 mM) at 4 h,
367 with an acetoin yield of 88.78% of the theoretical yield. In addition to acetoin, the
368 substrate ethanol and intermediate acetaldehyde were measured during the reaction.
369 The substrate ethanol was rapidly consumed and 6.25 mM residual ethanol remained
370 in the reaction solution at 4 h. Acetaldehyde accumulated up to 9.58 mM during the
371 first 2 h of the reaction, and then decreased to 5.65 mM at 6 h. No accumulation of
372 other undesired by-products was detected, indicating that the artificial synthetic
373 pathway was specific for the substrate. Subsequently, the effects of substrate
374 concentrations (200, 300, 400, and 500 mM) on acetoin production were investigated
375 using the optimized reaction mixture. As shown in Fig. 4B, the acetoin concentration
376 was increased by increasing the initial substrate concentration. A maximum acetoin
377 concentration of 117.5 mM was achieved at an ethanol concentration of 400 mM after
378 6 h. However, acetoin yield was only 58.71% of its theoretical yield. The intermediate
379 acetaldehyde showed significant accumulation when the initial ethanol concentration
380 was increased, suggesting that the FLS:L482S enzyme limits the productivity of this
381 CFME-based artificial pathway.

382

383 **2,3-Butanediol production from ethanol via artificial pathway**

384 **NAD(P)H purge valve regulatory node to prevent NADH buildup.**
385 Subsequently, we investigated 2,3-butanediol production from ethanol with the
386 enzyme BDH added to the CFME system. However, the artificial pathway from

387 ethanol to 2,3-butanediol generates more reducing equivalents than is required to
388 produce 2,3-butanediol (1 NADH per ethanol, with 0.5 NADH required). Herein, we
389 designed a NAD(P)H purge valve regulatory node to prevent the buildup of NADH.
390 As shown in Fig. 1B, we developed the mutant enzyme EtDH (D46G) to
391 simultaneously utilize NAD^+ and NADP^+ as coenzymes in the conversion of ethanol
392 to acetaldehyde by site-directed mutagenesis according to the results of sequence
393 alignment (Table 2 and Fig. S10†). Additionally, NADPH-dependent BDH^{1,29} from *C.*
394 *autoethanogenum* was used to catalyze acetoin into 2,3-butanediol in the presence of
395 NADPH. During the reaction process, NADH produced was rapidly recycled back to
396 NAD^+ via the H_2O -forming NOX, while NADPH generated was used to produce
397 2,3-butanediol from acetoin. When NADP^+ levels were high (NADPH low), the
398 mutant enzyme EtDH:D46G regenerated NADPH via the oxidation of ethanol.
399 However, when NADPH levels were high (NADP^+ low), BDH generated
400 2,3-butanediol from acetoin and regenerate NADP^+ without the buildup of additional
401 reducing equivalents (NADH produced from ethanol to acetaldehyde immediately
402 recycled for purging the excess). To achieve high catalytic efficiency, the mutant BDH
403 enzyme (S199A) was developed via site-specific mutagenesis as reported
404 previously.³⁵

405 **Characterization of mutants EtDH and BDH in the artificial pathway.** As
406 shown in Table 2 and Table S2†, the wild-type EtDH enzyme only employed NAD^+ as
407 a coenzyme for ethanol oxidation with $17.09 \text{ s}^{-1} \text{ mM}^{-1}$ of the $k_{\text{cat}}/K_{\text{m}}$ value, whereas its
408 variant EtDH:D46G simultaneously used NAD^+ and NADP^+ as coenzymes and the
409 $k_{\text{cat}}/K_{\text{m}}$ values for ethanol with NAD^+ and NADP^+ were 9.97 and $1.65 \text{ s}^{-1} \text{ mM}^{-1}$,
410 respectively. Compared with the wild-type NADPH-dependent BDH enzyme, the
411 $k_{\text{cat}}/K_{\text{m}}$ value of its variant BDH:S199A for acetoin with NADPH was up to 19.31 s^{-1}

412 mM⁻¹ (Table 2 and Table S2†). In addition, the enzyme thermostability of
413 EtDH:D46G and BDH:S199A was assayed at 30, 37, and 45 °C. EtDH:D46G activity
414 levels of 86.53% and 86.67% were retained after incubation at 30°C for 6 h when
415 acetaldehyde was used as a substrate with the coenzymes NAD⁺ and NADP⁺,
416 respectively (Fig. S5†). For the BDH:S199A enzyme, 80.81% of the initial enzyme
417 activity for acetoin with the coenzyme NADPH was retained at 30 °C for 6 h (Fig.
418 S5†).

419 2,3-Butanediol production from ethanol via improved artificial pathway.

420 The four enzymes, EtDH:D46G, FLS:L482S, BDH:S199A, and NOX, were reacted
421 with ethanol in the presence of 1 mM NAD⁺ and/or 1 mM NADP⁺. As shown in Fig.
422 S11†, no 2,3-butanediol was detected when NAD⁺ was used as a coenzyme in the
423 reaction system. This was primarily because BDH is an NADPH-dependent enzyme
424 in the conversion of acetoin to 2,3-butanediol. In contrast, 18.20 mM 2,3-butanediol
425 was produced from 100 mM ethanol as a substrate in the presence of NADP⁺,
426 indicating that NADP⁺ is required for 2,3-butanediol production in the artificial
427 cascade reaction. When 1 mM NAD⁺ and 1 mM NADP⁺ were simultaneously used in
428 the reaction, a maximum 2,3-butanediol concentration of 44.14 mM at 88.28 % of the
429 theoretical yield was produced from 100 mM ethanol after 5 h (Fig. 5A). The result
430 showed that use of the NAD(P)H purge valve regulatory node for preventing the
431 buildup of NADH was feasible and efficient. Throughout the reaction process, low
432 levels of acetoin accumulated in the reaction solution, demonstrating high catalytic
433 efficiency from acetoin to 2,3-butanediol by BDH:S199A (Fig. 5A). Furthermore,
434 different substrate concentrations were used to investigate the effects on
435 2,3-butanediol production in the reaction pathway. The maximum 2,3-butanediol
436 concentration was 127.3 mM when the initial ethanol concentration in the reaction

437 mixture was 500 mM (Fig. 5B). However, 2,3-butanediol yield decreased with
438 increasing initial ethanol concentration, although higher 2,3-butanediol concentration
439 was obtained. Analysis of the intermediates in the reaction solution revealed
440 accumulation of a large amount of acetaldehyde in the reaction system, indicating that
441 the conversion of acetaldehyde to acetoin by the FLS:L482S enzyme remained the
442 rate-limiting step. Compared with the results for acetoin production from ethanol, the
443 concentration of acetaldehyde in the 2,3-butanediol production system was
444 significantly decreased (Fig. 4B and Fig. 5B), suggesting that FLS:L482S enzyme
445 activity is partially inhibited by the product acetoin. However, the relatively low
446 catalytic efficiency of the FLS:L482S enzyme remained the major cause of
447 acetaldehyde accumulation.

448

449 **2-Butanol production from ethanol**

450 **Construction of an artificial pathway for 2-butanol production from ethanol.**

451 Finally, we employed an additional B₁₂-dependent DDH to convert
452 *meso*-2,3-butanediol into butanone,^{30,32,36} which can further be transformed into
453 2-butanol by BDH:S199A from *C. autoethanogenum* as shown in Fig. 1C.³⁵ Previous
454 studies showed that DDH enzyme with its reactivating factor dhaR from *L. brevis* was
455 the best candidate for catalyzing *meso*-2,3-butanediol into butanone *in vivo*.¹ To
456 determine its reaction conditions *in vitro*, the effects of four factors including
457 coenzyme B₁₂, ATP, Mg²⁺, and dhaR on the conversion of *meso*-2,3-butanediol to
458 butanone by DDH were investigated. The results suggested that the coenzyme B₁₂
459 and ATP were required for the catalytic reaction, whereas dhaR and Mg²⁺ efficiently
460 enhanced butanone production from *meso*-2,3-butanediol (Table S3†). Therefore,
461 coenzyme B₁₂, ATP, Mg²⁺, and dhaR were supplemented into the artificial reaction

462 pathway for efficient butanone production from *meso*-2,3-butanediol. To convert
463 butanone to 2-butanol, the BDH:S199A enzyme was used because it can reduce
464 acetoin and butanone into 2,3-butanediol and 2-butanol, respectively.³⁵ As shown in
465 Table 2 and Table S2†, the BDH:S199A enzyme showed high catalytic efficiency for
466 the substrate butanone with NADP^+ ($k_{\text{cat}}/K_m = 37.76 \text{ s}^{-1} \text{ mM}^{-1}$), which was improved
467 by 145.0% compared to wild-type BDH. Considering that 2-butanol exists in two
468 forms (*R*-2-butanol and *S*-2-butanol), we also analyzed the configuration of the
469 product from butanone by BDH:S199A. As shown in Fig. S16†, *R*- and *S*-2-butanol in
470 a ratio of 1.23:1 were produced from butanone by BDH:S199A at 30 °C after 6 h.

471 Theoretically, two moles of ethanol are oxidized to generate two moles of
472 reducing equivalents, which satisfies the need for the reduction of acetoin and
473 butanone into 2,3-butanediol and 2-butanol in the artificial pathway (Fig. 1C).
474 However, the DDH enzyme only catalyzed *meso*-2,3-butanediol into butanone,
475 whereas (*2R,3R*)-butanediol and (*2S,3S*)-butanediol are not substrates for DDH (Fig.
476 S4†). Thus, reducing equivalents would be excessive if the products from acetoin by
477 BDH were other forms of 2,3-butanediol except *meso*-2,3-butanediol. Therefore, the
478 configurations of acetoin and 2,3-butanediol were determined using a GC system
479 equipped with a chiral column. Chiral analysis indicated that 2,3-butanediol generated
480 from ethanol contained *meso*-2,3-butanediol (65%) and (*2R,3R*)-butanediol (35%)
481 from (*3S*)-acetoin and (*3R*)-acetoin, which were produced from acetaldehyde by
482 FLS:L482S (Fig. S14† and Fig. S15†). Considering that only *meso*-2,3-butanediol
483 was converted into butanone by DDH,³⁴ we used the same strategy for 2-butanol
484 production as 2,3-butanediol production from ethanol by employing an NAD(P)H
485 purge valve regulatory node to prevent the buildup of NADH (Fig. 1C).

486 **Rate limiting step for 2-butanol production from ethanol.** The reaction for

487 2-butanol production was carried out to determine the rate-limiting step using
488 EtDH:D46G, FLS:L482S, BDH:S199A, DDH with its reactivating factor dhaR, and
489 NOX enzymes. The rate-limiting experiment showed that only 1.84 mM 2-butanol
490 with a significant decrease of 79.16% was obtained from 100 mM ethanol when 1/10
491 concentration of the DDH enzyme was used, whereas lowering the concentration of
492 BDH:S199A to 10% had a little effect on 2-butanol production (Fig. 6A). This
493 demonstrates that DDH became a potential rate-limiting factor in the artificial reaction
494 for 2-butanol production. Based on previous studies,^{1,30} S302A, Q337A, F375I, and
495 their combinatorial variants in the DDH enzyme were developed by site-directed
496 mutagenesis. The results of whole-cell catalysis indicated that the mutant Q337A and
497 F375I DDH enzymes with dhaR produced 27.20 and 25.63 mM butanone from 50
498 mM *meso*-2,3-butanediol, while 19.76 mM butanone was obtained using the wild-type
499 DDH enzyme with dhaR. Furthermore, a maximum butanone concentration of 30.35
500 mM, which was an increase of 53.60%, was observed by the combinatorial variant of
501 DDH:Q337A/F375I with its reactivating factor dhaR (Fig. 6B and Fig. S12†).

502 Computational analysis showed that proton donor residue E171 of the double
503 mutant DDH (Q337A/F375I) (1.9Å) contacted the substrate 2,3-butanediol more
504 strongly than the wild-type (2.6Å) (Fig. S13A-B†). E171 showed more hydrogen
505 bond contacts with the substrate in the double mutant compared to the wild-type.
506 Long-range simulation (100 ns) results also showed that the substrate had stronger
507 interaction networks including hydrogen bonding and water bridges with E171 in the
508 double mutant compared to in the wild-type (Fig. S13C-D†).

509 **2-Butanol production from ethanol by improved artificial pathway.**
510 DDH:Q337A/F375I with dhaR rather than wild-type DDH was used to perform the
511 cascade reaction from ethanol to 2-butanol (Fig. 1C). As shown in Fig. 7, 13.62 mM

512 2-butanol at 27.24% of the theoretical yield was produced from 100 mM ethanol after
513 6 h in the cell-free bio-system. Furthermore, high levels of 2,3-butanediol (up to 32.55
514 mM) accumulated in the reaction solution, whereas butanone was not detected during
515 the reaction process. These results indicate that the conversion of 2,3-butanediol to
516 butanone by DDH:Q337A/F375I was a rate-limiting step. Although the whole-cell
517 biocatalyst co-expressing the DDH:Q337A/F375I enzyme and its reactivating factor
518 dhaR exhibited higher catalytic efficiency for the conversion of *meso*-2,3-butanediol
519 (50 mM) to butanone (30.35 mM), the *in vitro* enzyme activity assay showed a low
520 specific activity of 0.05 U mg⁻¹ for *meso*-2,3-butanediol (Table S2† and Fig. 6B). The
521 thermal instability of the DDH:Q337A/F375I enzyme also limited the conversion of
522 2,3-butanediol to butanone. As shown in Fig. S5†, the DDH:Q337A/F375I enzyme
523 only retained 1.21% of its initial activity after incubation at 30°C for 6 h, and no
524 activity was observed when the enzyme was incubated at 37 and 45°C for 6 h. During
525 the reaction process, 2-butanol production rapidly increased during the first 4 h and
526 then stopped increasing after 5 h, likely because of inactivation (Fig. 7). Therefore,
527 further improving the enzyme activity and stability of DDH by protein engineering or
528 searching for a new enzyme with high catalytic efficiency to convert 2,3-butanediol to
529 butanone would improve 2-butanol yield in the artificial synthetic pathway.

530

531 **Recyclability of cascade reactions**

532 The recyclability of the catalytic system is an attractive parameter that dictates
533 the economic feasibility of using these enzymes in the cell-free bio-system. To
534 evaluate the recyclability of the catalytic system, the enzymes for acetoin production
535 (EtDH, FLS:L482S, and NOX) and 2,3-butanediol production (EtDH:D46G,
536 FLS:L482S, BDH:S199A, and NOX) were immobilized on glutaraldehyde-

537 functionalized silicon oxide nanoparticles.^{37,38} Immobilized enzymes showed more
538 than 90% immobilization efficiency. Acetoin production by the immobilized enzymes
539 was evaluated and a recyclability test of the catalytic system was performed (Fig. 8).
540 Enzymes immobilized on silicon oxide nanoparticles exhibited 94% of their initial
541 product concentrations, even after 10 cycles of reuse to produce acetoin. This
542 indicates that there was no significant decrease in acetoin production using the
543 immobilized enzymes during repeated use. Additionally, the enzymes immobilized on
544 silicon oxide nanoparticles were stable because of the covalent linkages between the
545 enzymes and silicon oxide nanoparticles. Similarly, 2,3-butanediol production by
546 immobilized enzymes and recyclability of the catalytic system were evaluated (Fig. 8).
547 Here, the immobilized enzymes exhibited 73% of their initial 2,3-butanediol
548 production activity after 10 cycles of reuse. Upon immobilization, biocatalysts
549 catalyzed the production of acetoin and 2,3-butanediol for many cycles without
550 significant losses of activity. Hence, the immobilized catalytic system can be
551 efficiently recycled for industrial production of acetoin and 2,3-butanediol.
552 Unfortunately, we were not able to produce 2-butanol under the same experimental
553 conditions because of the low stability of DDH.

554 In recent years, acetoin, 2,3-butanediol, and 2-butanol as platform chemicals
555 have gained more attention because of their increasing market demands. The
556 derivatives of 2,3-butanediol have a potential global market of approximately 32
557 million tons per annum.²⁹ As a precursor of 2,3-butanediol, acetoin has been classified
558 as one of the 30 platform chemicals that are given priority for development and
559 utilization by the US Department of Energy, and its market demand has reached more
560 than 10 kilotons per annum,³⁹ while the market capacity of bio-butanol is
561 approximately 5 million tons per annum.⁴⁰ Previous studies have shown that acetoin

562 and 2,3-butanediol could be produced by microbial fermentation or chemical
563 synthesis.^{39,41} Compared to chemical synthesis, microbial fermentation for acetoin and
564 2,3-butanediol production has attracted greater attention due to its mild condition.
565 However, during the fermentation process, many metabolic byproducts are inevitably
566 produced, resulting in difficulty in product isolation and high purification cost. In
567 addition, the resulting microbial biomass causes environmental problems.
568 Commercially available 2-butanol is primarily obtained industrially by the hydration
569 of 1-butene using sulfuric acid as a catalyst. However, the harsh reaction condition
570 results in higher cost for 2-butanol production and potential environmental pollution.
571 Compared to chemical synthesis and microbial fermentation, the artificial
572 multi-enzyme pathway in the current work provides an environment-friendly, fewer
573 byproduct-forming, and recyclable process with high conversion efficiency, thus
574 supporting the viability of producing acetoin, 2,3-butanediol, and 2-butanol from
575 ethanol by CFME.

576

577 **Conclusions**

578 In conclusion, we developed an artificial multi-enzyme pathway capable of
579 upgrading ethanol to C₄ compounds (Table 3). High activity (>88% conversion) was
580 obtained for acetoin or 2,3-butanediol production from ethanol. Additionally, the
581 artificial synthetic pathway showed potential for butanone and 2-butanol production,
582 although their yields were relatively low because of the low activity and stability of
583 DDH enzyme. This environmentally friendly novel approach can be used to upgrade
584 bio-ethanol to acetoin, 2,3-butanediol, and 2-butanol. Ongoing efforts are focused on
585 developing modified FLS and DDH enzymes with high catalytic efficiency as well as
586 identifying new enzymes. Overall, this artificial CFME approach is a promising and

587 highly selective strategy for ethanol-to-C₄ compounds conversion using our novel
588 cascade enzymes system.

589

590 **Acknowledgements**

591 This work was supported by the National Natural Science Foundation of China
592 (No. 81673542), New Century Excellent Talents Supporting Plan of the Provincial
593 Education Department of Fujian Province of China (No. K8015056A), the
594 Development Platform of Edible Fungi Industry in Fujian Province (No. K5114001A),
595 and Basic Science Research Program through the National Research Foundation of
596 Korea (NRF) funded by the Ministry of Science, ICT & Future Planning
597 (2017R1A2B3011676, 2017R1A4A1014806, 2013M3A6A8073184).

598

599 **References**

- 600 1 Z. Chen, Y. Wu, J. H. Huang, and D. H. Liu, *Bioresource Technol.*, 2015, **197**,
601 260.
- 602 2 H. Latif, A. A. Zeidan, A. T. Nielsen and K. Zengler, *Curr. Opin. Biotechnol.*,
603 2014, **27**, 79.
- 604 3 A. S. Heeres, C. S. Picone, L. A. van der Wielen, R. L. Cunha and M. C. Cuellar,
605 *Trends Biotechnol.*, 2014, **32**, 221.
- 606 4 C. Gao, Z. Li, L. J. Zhang, C. Wang, K. Li, C. Q. Ma, and P. Xu, *Green Chem.*,
607 2015, **17**, 804.
- 608 5 M. Simoes, S. Baranton and C. coutanceau, *ChemSusChem*, 2012, **5**, 2106.
- 609 6 A. J. Ragauskas, C. K. Williams, B. H. Davison, G. Britovsek, J. Cairney, C. A.
610 Eckert, W. J. Frederick, J. P. Hallett, D. J. Leak, C. L. Liotta, J. R. Mielenz, R.
611 Murphy, R. Templer and T. Tschaplinski, *Science*, 2006, **311**, 484.

- 612 7 K. N. Tseng, S. Lin, J. W. Kampf and N. K. Szymczak, *Chem. Comm.*, 2016, **52**,
613 2901.
- 614 8 S. Manzetti and O. Andersen, *Fuel*, 2015, **140**, 293.
- 615 9 P. Dürre, *Biotechnol. J.*, 2007, **12**, 1525.
- 616 10 V. García, J. Pääkilä, H. Ojamo, E. Muurinen, and R. L. Keiski, *Renewable*
617 *Sustainable Energy Rev.*, 2011, **2**, 964.
- 618 11 E. I. Lan, and J. C. Liao, *Bioresource Technol.*, 2013, **135**, 339.
- 619 12 P. P. Peralta-Yahya, F. Zhang, S. B. Del Cardayre, J. D. Keasling, *Nature*, 2012,
620 **7411**, 320.
- 621 13 L. X. Li, K. Li, Y. Wang, C. Chen, Y. Q. Xu, L. J. Zhang, B. B. Han, C. Gao, F.
622 Tao, C. Q. Ma, and P. Xu, *Metab. Eng.*, 2016, **28**, 19.
- 623 14 L. Y. Zhang, Y. L. Yang, J. A. Sun, Y. L. Shen, D.Z. Wei, J.W. Zhu, and J. Chu,
624 *Bioresource Technol.*, 2010, **101**, 1961.
- 625 15 N. Li, W. J. Yan, P. J. Yang, H. X. Zhang, Z. J. Wang, J. F. Zheng, S. P. Jia and Z.
626 P. Zhu, *Green Chem.*, 2016, **18**, 6029.
- 627 16 P. Ghiaci, J. Norbeck, and C. Larsson, *Plos one*, 2014, **9**, e102774.
- 628 17 D. Cai, Y. Wang, C. J. Chen, P. Y. Qin, Q. Miao, C. W. Zhang, P. Li and T. W. Tan,
629 *Bioresource Technol.*, 2016, **211**, 704.
- 630 18 P. S. Nigam, A. Singh, *Prog. Energy Combust. Sci.*, 2011, **37**, 52.
- 631 19 A. Baez, K. M. Cho, and J. C. Liao, *Appl. Microbiol. Biotechnol.*, 2011, **90**, 1681.
- 632 20 C. R. Shen, E. I. Lan, Y. Dekishima, A. Baez, K. M. Cho and J. C. Liao, *Appl.*
633 *Environ. Microbiol.*, 2011, **77**, 2905.
- 634 21 B. R. Oh, S. Y. Heo, S. M. Lee, W. K. Hong, J. M. Park, Y. R. Jung, D. H. Kim, J.
635 H. Sohn, J. W. Seo, and C. H. Kim, *Biotechnol. Lett.*, 2014, **36**, 57.
- 636 22 Q. M. Dudley, A. S. Karim and M. C. Jewett, *Biotechnol. J.*, 2015, **10**, 69.

- 637 23 W. D. Fessner, *New Biotechnol.*, 2015, **32**, 658.
- 638 24 C. You, H. Chen, S. Myung, N. Sathitsuksanoh, H. Ma, X. Z. Zhang, J. Li and Y.
639 H. Zhang, *Proc. Natl. Acad. Sci. U. S. A.*, 2013, **110**, 7182.
- 640 25 J. S. Martín del Campo, J. Rollin, S. Myung, Y. Chun, S. Chandrayan, R. Patiño,
641 M. W. Adams and Y. H. Zhang, *Angew. Chem. Int. Ed.*, 2013, **52**, 4587.
- 642 26 S. Myung, J. Rollin, C. You, F. Sun, S. Chandrayan, M. W. Adams and Y. H.
643 Zhang, *Metab. Eng.*, 2014, **24**, 70.
- 644 27 T. Y. Wu, C. T. Chen, J. T. Liu, I. W. Bogorad, R. Damoiseaux and J. C. Liao,
645 *Appl. Microbiol. Biotechnol.*, 2016, **100**, 1.
- 646 28 J. Siegel, A. L. Smith, S. Poust, A. Wargacki, A. Bar-Even, C. Louw, B. Shen, C.
647 Eiben, H. Tran, E. Noor, J. Gallaher, J. Bale, Y. Yoshikuni, M. Gelb, J. Keasling,
648 B. Stoddard, M. Lidstrom and D. Baker, *Proc. Natl. Acad. Sci. U. S. A.*, 2015, **112**,
649 3704.
- 650 29 M. Köpke, M. L. Gerth, D. J. Maddock, A. P. Mueller, F. M Liew, S. D. Simpson,
651 *Appl. Environ. Microbiol.*, 2014, **80**, 3394.
- 652 30 M. Yamanishi, K. Kinoshita, M. Fukuoka, T. Saito, A. Tanokuchi, Y. Ikeda, H.
653 Obayashi, K. Mori, N. Shibata, T. Tobimatsu and T. Toraya, *FEBS. J.*, 2012, **279**,
654 793.
- 655 31 Y. W. Zhang, M. K. Tiwari, H. Gao, S. S. Dhiman, M. Jeya and J. K. Lee, *Enzyme*
656 *Microbiol. Tech.*, 2012, **50**, 255.
- 657 32 M. Seyfried, R. Daniel and G. Gottschalk, *J. Bacteriol.*, 1996, **178**, 5793.
- 658 33 J. Bendl, J. Stourac, E. Sebestova, O. Vavra, M. Musil, J. Brezovsky and J.
659 Damborsky, *Nucleic. Acids Res.*, 2016, **44**, 479.
- 660 34 Z. Chen, H. Sun, J. H. Huang, Y. Wu and D. H. Liu, *Plos ONE*, **2015**, 10,
661 e0140508.

- 662 35 D. J. Maddock, W. M. Patrick and M. L. Gerth, *Protein Eng. Des. Sel.*, 2015, **28**,
663 251.
- 664 36 S. Kwak, Y. C. Park and J. H. Seo, *Bioresource Technol.*, 2013, **135**, 432.
- 665 37 S. K. S. Patel, S. H. Choi, Y. C. Kang and J. K. Lee, *Nanoscale*, 2016, **8**, 6728.
- 666 38 S. K. S. Patel, S. H. Choi, Y. C. Kang and J. K. Lee. *ACS Appl Mater Inter*, 2017,
667 **9**, 2213.
- 668 39 L. J. Zhang, Q. Y. Liu, Y. S. Ge, L. X. Li, C. Gao, P. Xu, and C. Q. Ma, *Green*
669 *Chem.*, 2015, **18**, 1560.
- 670 40 G. R. Ding, B. Meng, R. L. Chen, and J. H. Chen, *Chem. Indust.*, 2016, **34**, 37.
- 671 41 Y. Q. Xu, H. P. Chu, C. Gao, F. Tao, Z. K. Zhou, K. Li, L. X. Li, C. Q. Ma, and P.
672 Xu, *Metab. Eng.*, 2014, **23**, 22.

Table 1 Bacterial strains and plasmids used in this study.

Strain or plasmid	Relevant genotype and description	source
Strains		
<i>E. coli</i> DH5 α	Host of plasmid for cloning	Lab stock
<i>E. coli</i> BL21(DE3)	Host of plasmid for expression, F ⁻ , ompT, hsdSB(rB-mB ⁻), gal(λ c I 857, ind1, Sam7, nin5, lacUV-T7 gene1), dcm(DE3)	Lab stock
Plasmids		
pET28a	Expression vector, Km ^R	Novagen
pET-EtDH	pET28a carries <i>EtDH</i> gene	This study
pET-EtDH:D46G	pET28a carries <i>EtDH</i> mutant gene	This study
pET-FLS	pET28a carries <i>FLS</i> gene	This study
pET-FLS:L482S	pET28a carries <i>FLS</i> mutant gene	This study
pET-FLS:L482R	pET28a carries <i>FLS</i> mutant gene	This study
pET-FLS:L482E	pET28a carries <i>FLS</i> mutant gene	This study
pET-BDH	pET28a carries <i>BDH</i> gene	This study
pET-BDH:S199A	pET28a carries <i>BDH</i> mutant gene	This study
pET-DDH	pET28a carries <i>DDH</i> gene	This study
pET-DDH:S302A	pET28a carries <i>DDH</i> mutant gene	This study
pET-DDH:Q337A	pET28a carries <i>DDH</i> mutant gene	This study
pET-DDH:F375I	pET28a carries <i>DDH</i> mutant gene	This study
pET-DDH:S302A/Q337A	pET28a carries <i>DDH</i> mutant gene	This study
pET-DDH:S302A/F375I	pET28a carries <i>DDH</i> mutant gene	This study
pET-DDH:Q337A/F375I	pET28a carries <i>DDH</i> mutant gene	This study
pET-DDH:S302A/Q337A/F375I	pET28a carries <i>DDH</i> mutant gene	This study
pET-dhaR	pET28a carries <i>dhaR</i> gene	This study
pET-DDH-dhaR	pET28a carries <i>DDH</i> and <i>dhaR</i> genes	This study
pET-NOX	pET28a carries <i>NOX</i> gene	This study

Table 2 Kinetic parameters of EtDH, FLS, BDH, and their variants.

Enzyme	Substrate/coenzyme	K_m (mM)	k_{cat} (s ⁻¹)	k_{cat}/K_m (s ⁻¹ mM ⁻¹)	References
EtDH	Ethanol/NAD ⁺	0.37 ± 0.05	6.28 ± 0.11	17.09	This study
	Ethanol/NADP ⁺	0	0	0	This study
EtDH:D46G	Ethanol/NAD ⁺	0.57 ± 0.03	5.65 ± 0.09	9.97	This study
	Ethanol/NADP ⁺	0.60 ± 0.02	0.99 ± 0.03	1.65	This study
FLS	Acetaldehyde/TPP	58.46 ± 2.32	0.45 ± 0.03	7.69 × 10 ⁻³	This study
FLS:L482S	Acetaldehyde/TPP	47.45 ± 1.20	0.63 ± 0.01	1.33 × 10 ⁻²	This study
FLS:L482R	Acetaldehyde/TPP	50.27 ± 1.44	0.53 ± 0.02	1.06 × 10 ⁻²	This study
FLS:L482E	Acetaldehyde/TPP	50.95 ± 1.51	0.49 ± 0.03	9.66 × 10 ⁻³	This study
BDH	Acetoin/NADPH	84.86 ± 7.98	157.0 ± 9.0	18.50	This study
	Acetoin/NADH	0	0	0	This study
	Butanone/NADPH	1.94 ± 0.05	29.90 ± 1.02	15.41	This study
	Butanone/NADH	0	0	0	This study
BDH:S199A	Acetoin/NADPH	116.1 ± 8.7	224.3 ± 9.7	19.31	This study
	Acetoin/NADH	0	0	0	This study
	Butanone/NADPH	1.08 ± 0.03	40.78 ± 1.42	37.76	This study
	Butanone/NADH	0	0	0	This study
DDH	2,3-butanediol/B12	10.4	35	3.4	36
NOX	O ₂ /NADH	5.8 × 10 ⁻³	218.7	3.77 × 10 ⁴	31

Table 3 Summary of acetoin, 2,3-butanediol, and 2-butanol production from 100 mM ethanol by cell free multi-enzyme catalysis

Product (mM)	Enzymes (U mL ⁻¹)	Chemicals (mM)	Yield (%)	Reaction time (h)
Acetoin (44.39)	EtDH (1.06), FLS:L482S (0.05), NOX (0.98)	NAD ⁺ (1), TPP (0.1), Mg ²⁺ (1), DTT (1)	88.78	4
2,3-BD (44.14)	EtDH:D46G (0.88), FLS:L482S (0.05), NOX (0.98), BDH:S199A (5.11)	NAD ⁺ (1), NADP ⁺ (1), TPP (0.1), Mg ²⁺ (1), DTT (1)	88.28	5
2-Butanol (13.62)	EtDH:D46G (0.88), FLS:L482S (0.05), NOX (0.98), BDH:S199A (5.11), DDH:Q337A/F375I (0.01)	NAD ⁺ (1), NADP ⁺ (1), TPP (0.1), Mg ²⁺ (1), DTT (1), coenzyme B ₁₂ (1), ATP (100)	27.24	6

All reactions were performed in 50 mM HEPES buffer (pH 8.0) and 20% DMSO using 100 mM EtOH as a substrate at 30 °C.

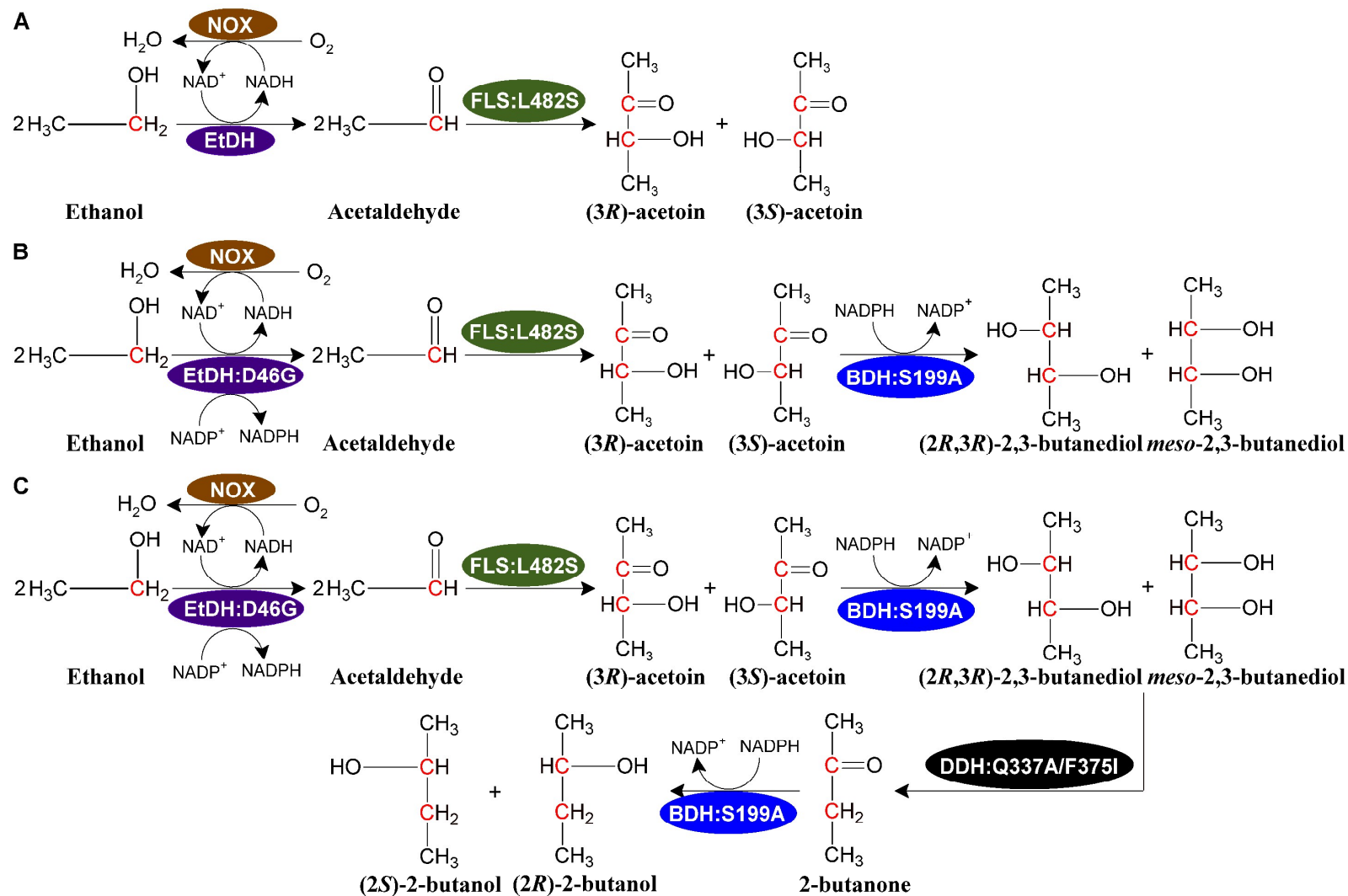


Fig. 1 Bio-system based on the artificial reaction cascade for the conversion of ethanol to acetoin (A), 2,3-butanediol (B), and 2-butanol (C). The enzymes are ethanol dehydrogenase (EtDH and its variant EtDH:D46G from *C. necator*), formolase (FLS:L482S, a newly designed enzyme originated from *P. fluorescens*), 2,3-butanediol dehydrogenase (BDH:S199A from *C. autoethanogenum*), diol dehydratase (DDH:Q337/F375I from *L. brevis*), and NADH oxidase (NOX from *L. rhamnosu*)

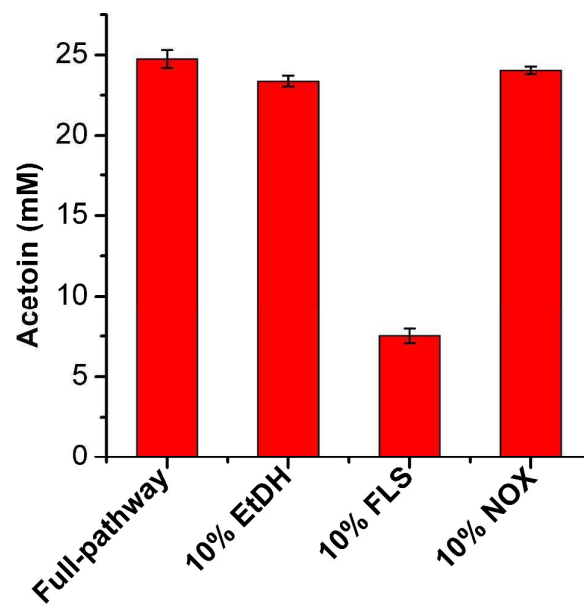


Fig. 2 Analysis of the rate-limiting step in the conversion of ethanol to acetoin. Results are the means \pm SD of three parallel replicates.

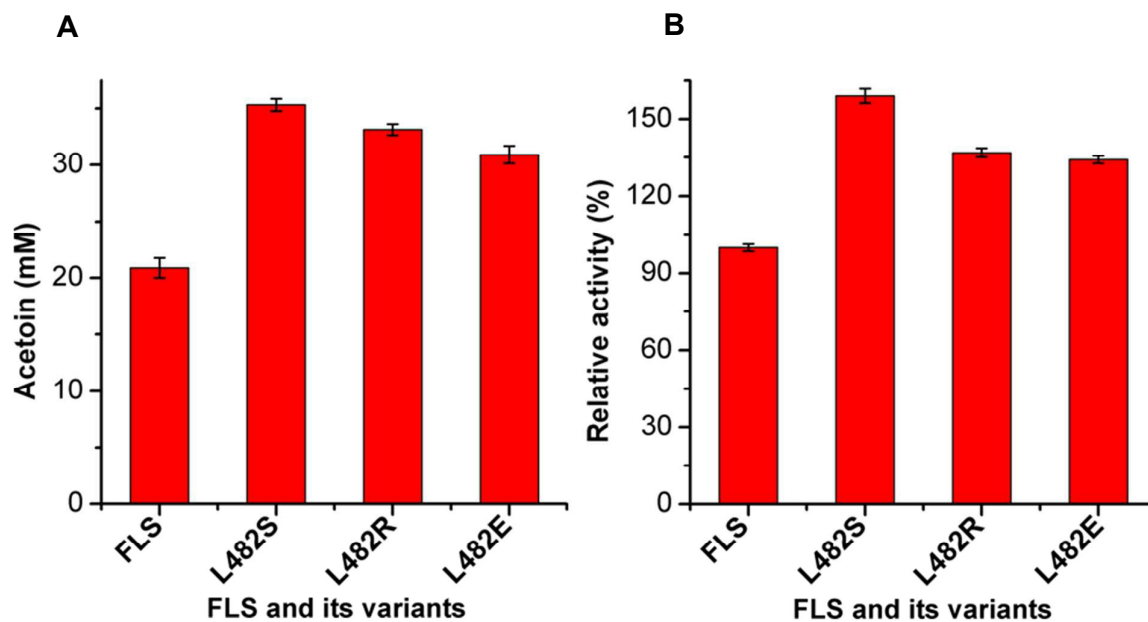


Fig. 3 Screening of positive FLS variants by whole-cell biocatalysis using acetaldehyde (100 mM) as a substrate (A) and activity assays of FLS and its variants after purification (B). A, The product acetoin from acetaldehyde through whole-cell biocatalysis was determined using the VP test; B, Percentage ratios were calculated based on specific activities (specific activity of FLS was 0.16 U/mg). Results are the means \pm SD of three parallel replicates.

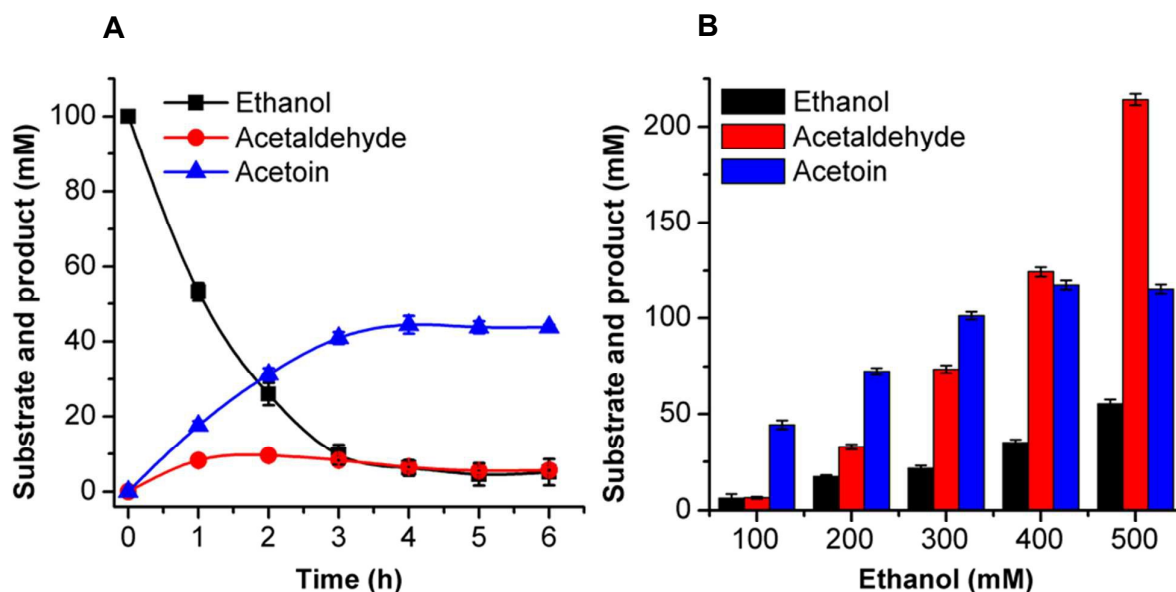


Fig. 4 Time-course of acetoin production from 100 mM ethanol (A) and effects of different substrate concentrations on acetoin production (B) by the artificial reaction cascade. A, The reaction was performed in a 0.5-mL reaction mixture containing 50 mM HEPES buffer (pH 8.0), 1 mM NAD^+ , 1.06 U mL^{-1} EtDH, 0.05 U mL^{-1} FLS:L482S, 0.98 U mL^{-1} NOX, 0.1 mM TPP, 1 mM Mg^{2+} , 1 mM DTT, 20% DMSO, and 100 mM ethanol; B, The reactions were carried out under the same conditions, except that the substrate concentration was 200–500 mM ethanol. These reactions were conducted at 30°C for 6 h. Results are the means \pm SD of three parallel replicates.

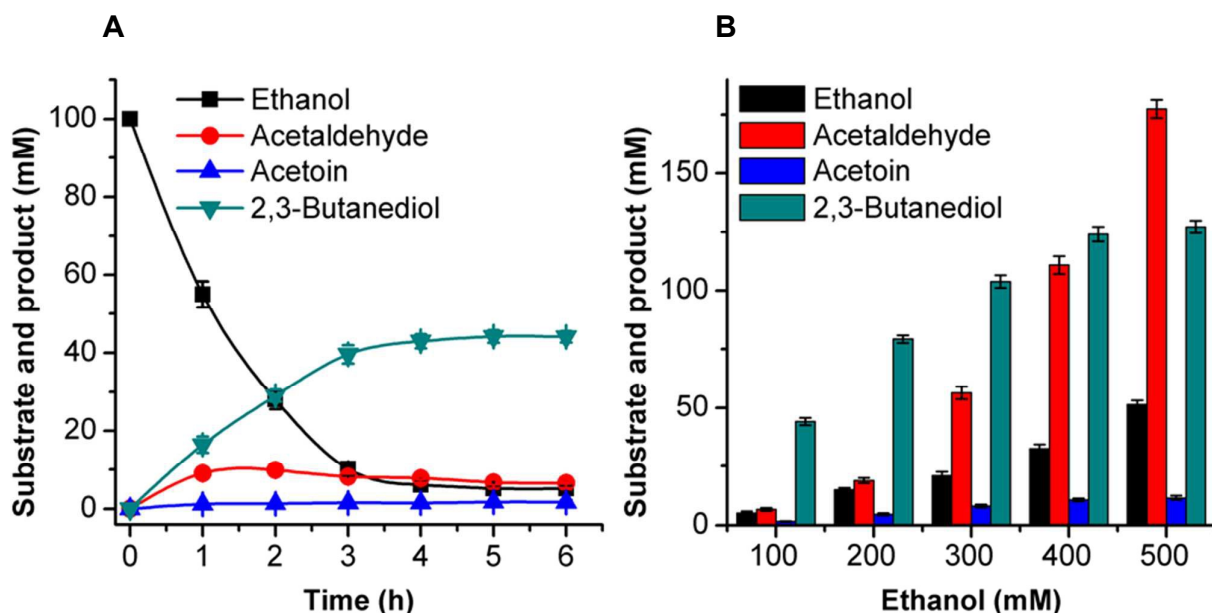


Fig. 5. Time-course of 2,3-butanediol production from 100 mM ethanol (A) and effects of different substrate concentrations on 2,3-butanediol production (B) by the artificial reaction cascade. A, The reaction was carried out in a 0.5-mL reaction mixture containing 50 mM HEPES buffer (pH 8.0), 1 mM NAD^+ , 1 mM NADP^+ , 0.88 U mL^{-1} EtDH:D46G, 0.05 U mL^{-1} FLS:L482S, 0.98 U mL^{-1} NOX, 5.11 U mL^{-1} BDH:S199A, 0.1 mM TPP, 1 mM Mg^{2+} , 1 mM DTT, 20% DMSO, and 100 mM ethanol; B, The reactions were carried out under the same conditions except that the substrate concentrations were 200–500 mM ethanol. These reactions were conducted at 30°C for 6 h. Results are the means \pm SD of three parallel replicates.

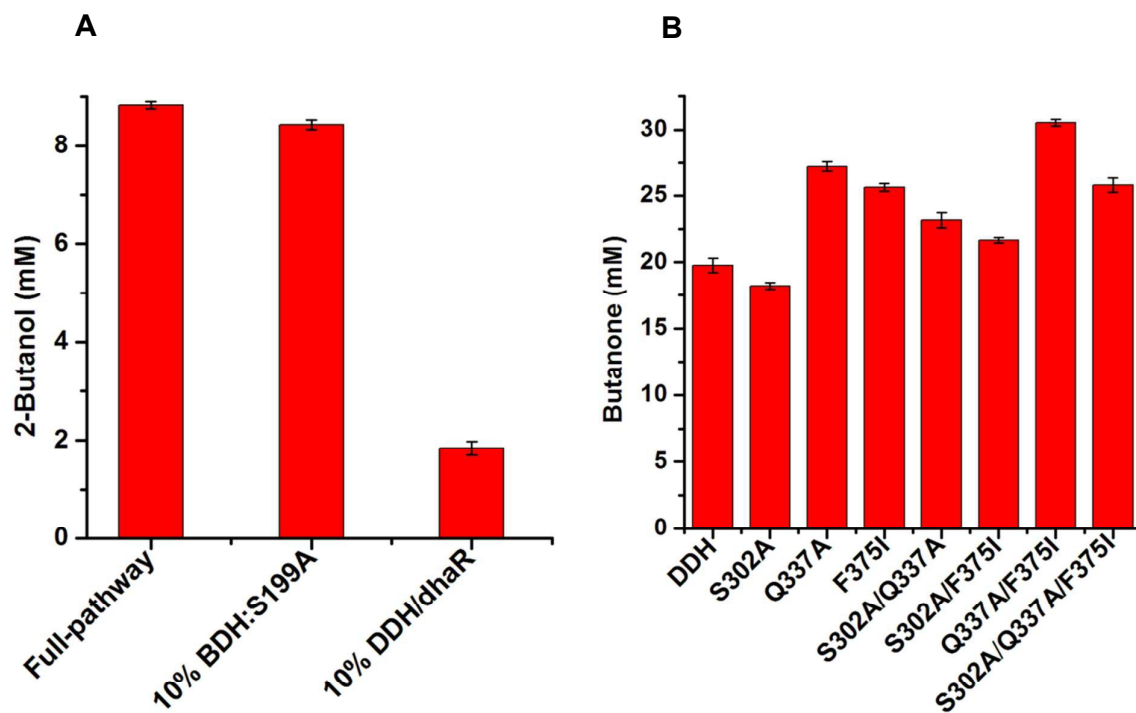


Fig. 6 Analysis of the rate-limiting step in the conversion of ethanol to 2-butanol (A). Catalytic efficiency assays of DDH enzyme and its variants with *meso*-2,3-butanediol (50 mM) as a substrate using whole-cell biocatalytic method (B). Results are the means \pm SD of three parallel replicates.

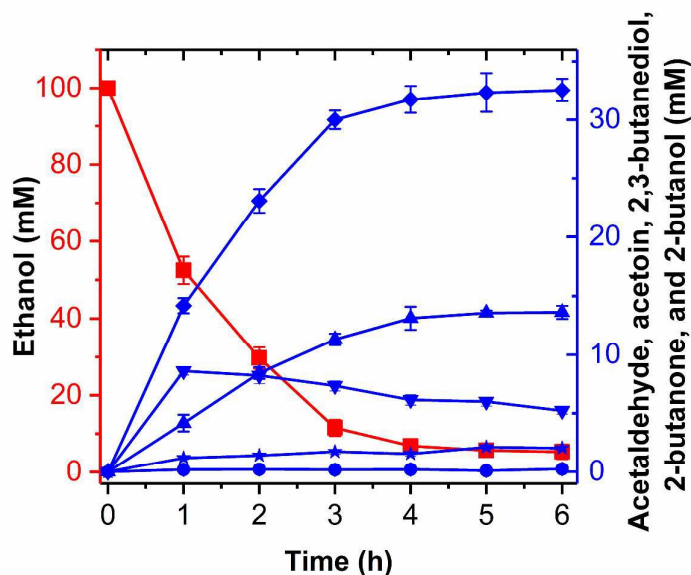


Fig. 7 Conversion of ethanol into 2-butanol by the artificial reaction cascade. Ethanol (square), acetaldehyde (inverted triangle), acetoin (circle), 2,3-butanediol (diamond), butanone (star), and 2-butanol (upright triangle). The reaction was carried out in a 0.5-mL reaction mixture containing 50 mM HEPES buffer (pH 8.0), 1 mM NAD⁺, 1 mM NADP⁺, 0.88 U mL⁻¹ EtDH:D46G, 0.05 U mL⁻¹ FLS:L482S, 0.98 U mL⁻¹ NOX, 5.11 U mL⁻¹ BDH:S199A, 0.01 U mL⁻¹ DDH:Q337A/F375I, 0.2 mg mL⁻¹ dhaR, 0.1 mM TPP, 1 mM Mg²⁺, 1 mM DTT, 20% DMSO, 1 mM coenzyme B₁₂, 100 mM ATP and 100 mM ethanol. The reaction was conducted at 30°C for 6 h. Results are the means ± SD of three parallel replicates.

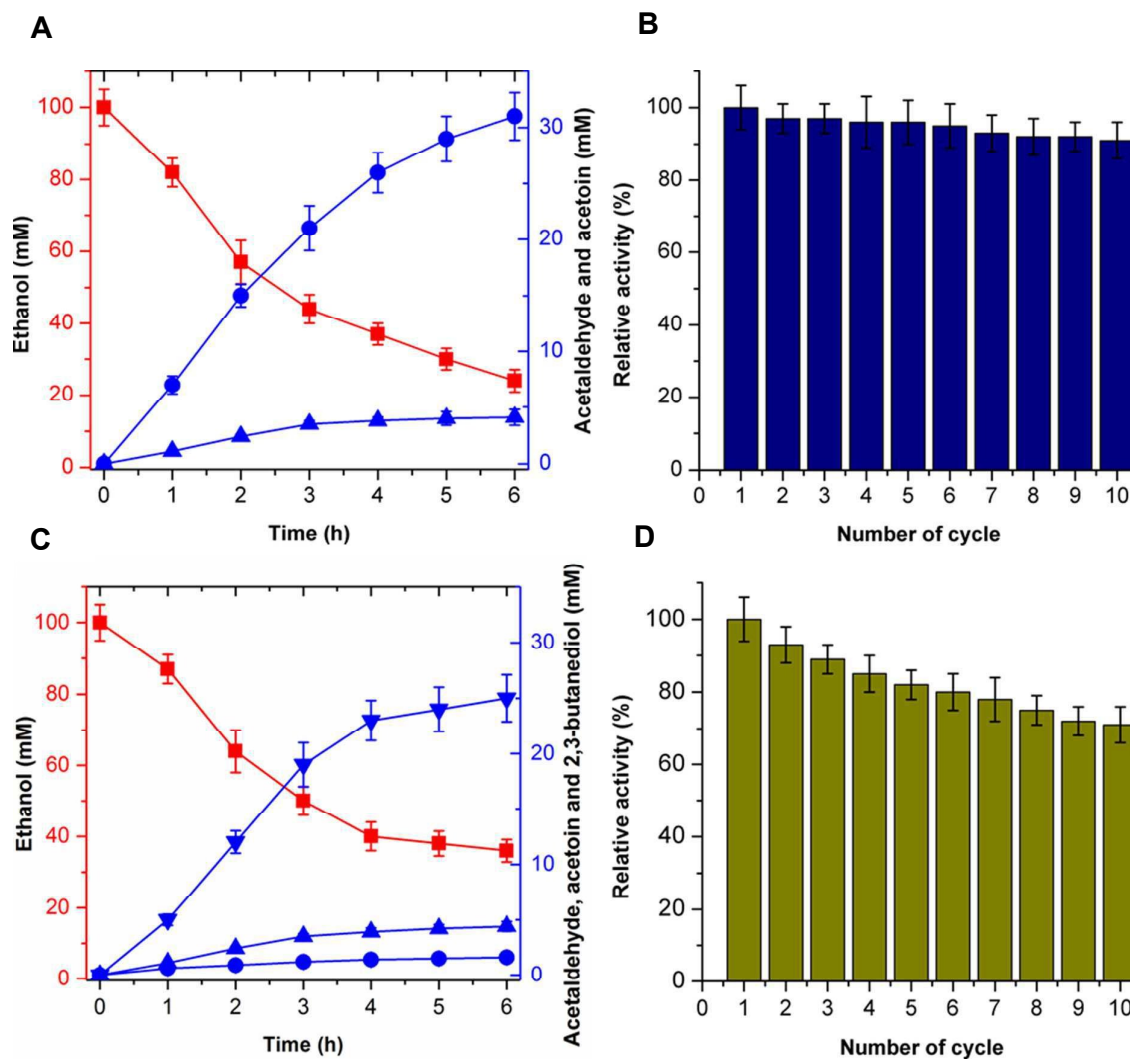


Fig. 8 Recyclability of the catalytic system. (A) Conversion of ethanol into acetoin by the artificial cascade reaction using immobilized enzymes. Ethanol (square), acetaldehyde (upright triangle), and acetoin (circle). (B) Reusability of the immobilized enzymes to produce acetoin from ethanol. (C) Conversion of ethanol into 2,3-butanediol by the artificial reaction cascade using immobilized enzymes. Ethanol (square), acetaldehyde (upright triangle), acetoin (circle), and 2,3-butanediol (inverted triangle). (D) Reusability of the immobilized enzymes to produce 2,3-butanediol from ethanol. The product concentration of the immobilized enzyme catalyzed reaction after the first cycle was set at 100%. Acetoin and 2,3-butanediol concentration were determined using a gas chromatograph system equipped with a chiral column (Supelco β -DEXTM 120, 30-m length, 0.25-mm inner diameter).